Mem. Fac. Sci. Eng. Shimane Univ.
Series A
32, pp. 1-17 (1998)

Crystal Growth of II–VI and I–III–VI_2 Compound Semiconductors by Chemical Transport 1. Transport Experiments

Yasutoshi NODA

Department of Material Science, Faculty of Science and Engineering, Shimane University
Nishikawatsu 1060, Matsue City, Shimane 690-8504, Japan

Yoshitaka FURUKAWA and Katashi MASUMOTO

Department of Materials Science, Faculty of Engineering, Tohoku University
Aoba-Aramaki, Sendai City, Miyagi 980-8579, Japan

(Received September 18, 1998)

Abstract

The chemical transport is one of the most important methods for crystal growth of compound semiconductors. In this study, the crystal growth by the chemical transport was applied to ZnSe of II–VI and $AgGaS_2$ of I–III–VI_2 compound semiconductors which have been expected as the material for optoelectronic devices. The growth of ZnSe and $AgGaS_2$ was made by using iodine and halides as the transport agent, where the growth parameters were source zone temperature, the temperature difference between source and growth zones, and amount of transport agent (M).

The transport rate plotted as a function of M showed the characteristic features. In case of ZnSe, the transport rate was divided into three regions of a gradual increase, a plateau and a steep increase with an increase of M, which resulted in fine granular, block form and needle-like crystals, respectively. In the case of $AgGaS_2$, the transport rate showed a maximum with an increase of M. The maximum transport rate increased in the order of Cl, Br and I in the transport agents. The crystal forms of rod and block were dependent on the transport rate.

The grown crystals were evaluated by measuring the photoluminescence (PL) spectra. All the ZnSe crystals only showed the self-activated emission peak indicating the presence of deep-level defects and nonradiative recombination centers. The spectra of the $AgGaS_2$ crystals were dependent upon the amount of iodine charged. With less amount of iodine, the crystals exhibited clear excitonic emissions, which means good quality of the crystal. The nonradiative recombination centers were increasingly introduced with an increase in the amount of transport agents.

1. Introduction

Zinc blend type II–VI and chalcopyrite type I–III–VI_2 compound semiconductors are expected as materials for optoelectronic devices. ZnSe is a wide-gap semiconductor (band gap

energy, E_g=2.7 eV† at 4.2 K) and has been studied as the material for optoelectronic devices in the blue-light region[1], while $AgGaS_2$ has a direct-transition band structure with E_g=2.73 eV[2,3] at 4.2 K and is expected as the material for non-linear optics[4-9].

The bulk crystal growth for ZnSe has been performed mainly on the basis of (i) high pressure melt growth[10,11], (ii) sublimation[12], (iii) chemical transport[13] and (iv) flux method[14]. In the vertical chemical transport system, the large size ZnSe single crystal was obtained and the morphologies of the grown crystals were investigated under the optimum growth condition, where the growth was limited by thermal convection[15].

The growth of $AgGaS_2$ single crystals has almost based on melt-growth technique[16-21]. The preliminary crystal growth by chemical transport was already reported for $AgGaS_2$[22,23], but the quality of the grown crystals was not investigated.

The crystal growth from the vapor phase is essential for both bulk crystals of good-quality and epitaxial thin films. The chemical transport has the advantages of low growth temperature, high growth rate and simple growth apparatus. In the present study, the chemical transport of ZnSe and $AgGaS_2$ was performed in a horizontal closed system and pursued the condition for growing large and good quality single crystals. The quality of the grown crystals was evaluated by photoluminescence measurement.

2. Chemical Transport of ZnSe

2.1 Experimental

The polycrystalline ZnSe as the source material was synthesized by the direct reaction of the constituent elements; Zn and Se at nominal purity of 99.9999%. Iodine was adopted as the transport agent which was special-class grade(99.8% with 0.03% Cl and 0.01% SO_4).

Figure 1 shows the chemical transport apparatus. The polycrystals were vacuum-sealed in

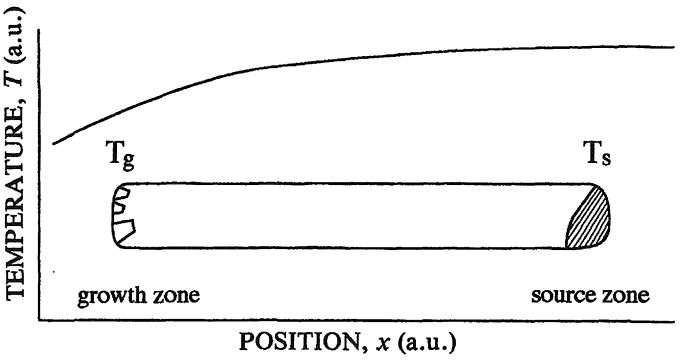

Fig. 1. Schematic diagram of chemical transport apparatus.

† 1 eV=1.60×10⁻¹⁹ J

the transparent quartz ampoule with the weighed amount of the iodine, which was cooled at one end in the ampoule with ice-water to diminish evaporation loss on evacuation. The dimension of the ampoule was 8 mm in inner diameter and 100 mm in length. The transport experiment was performed under the conditions: amount of iodine; $M=0.10\sim30$ kg/m^3, heating temperature of the source zone; $T_s=1098\sim1223$ K, that of the growth zone; $T_g=1073\sim1173$ K, $\Delta T(=T_s-T_g)=25\sim50$ K and growth period; $t=24\sim75$ hr. After the heating, the ampoule was air-cooled. No crystal grew midway between the source and the growth zones. The crystals grown at the growth zone were cleansed by acetone from iodine deposited on their surfaces.

2.2 Transport Rate

The transport rate was estimated by weighing the total amount of the grown crystals. Figure 2 shows the relationship between observed transport rate (N_0) and M for a variety of temperatures. Under the condition of $T_s=1098$ and $T_g=1073$ K, the rate at $M<1.0$ kg/m^3 showed a gradual increase with an increase of M, a plateau at $M=1.0\sim5.0$ kg/m^3 and a steep increase at $M>5.0$ kg/m^3. In the plateau region, N_0 was about 10^{-9} kg/s, which was by about 10^2 times larger than that measured in the case of $M=0.0$ kg/m^3 (sublimation method). Thus, the transport rate was enhanced through the transport reactions under the same heating conditions.

Figure 3 shows the crystals grown at $T_s=1098$ and $\Delta T=25$ K. The fine granular crystals

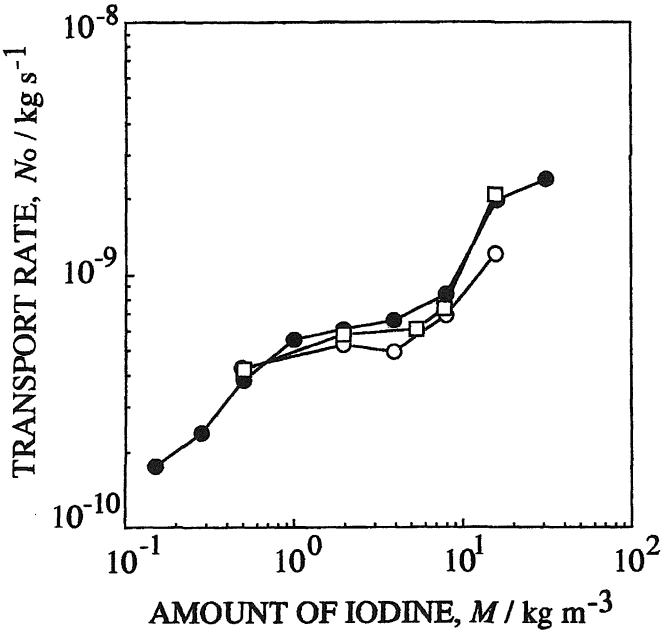

Fig. 2. Observed transport rate of ZnSe plotted against amount of iodine. The growth conditions: (●); $T_s=1098$ K and $\Delta T=25$ K, (○); $T_s=1123$ K and $\Delta T=25$ K, (□); $T_s=1123$ K and $\Delta T=50$ K.

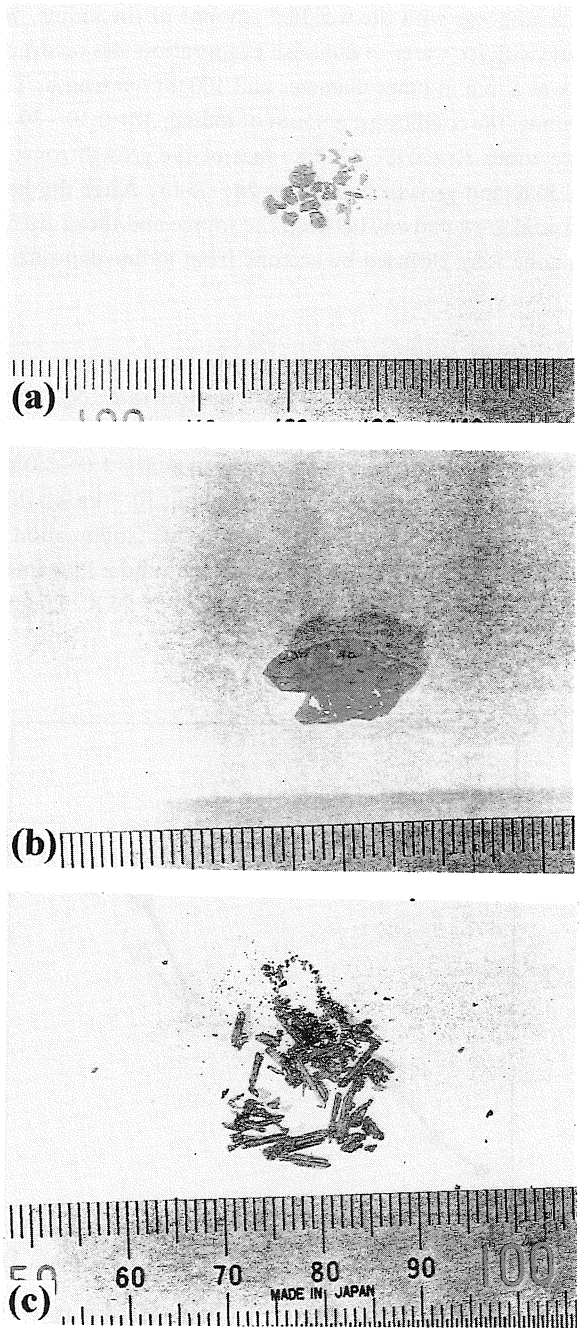

Fig. 3. ZnSe crystals grown at $T_s=1098$ K and $\Delta T=25$ K, with $M=$ (a) 1.0, (b) 5.0 and (c) 16 kg/m^3. 1 div. = 1 mm.

less than 1 mm in diameter resulted at $M<1.0$ kg/m^3. In the plateau region, the crystals had well-developed habit planes, the dimensions of which were $1\times1\times0.5$ mm^3 at $M=1.0$ kg/m^3 and increased with an increase of M. The largest single crystal with the dimension of $10\times5\times3$ mm^3 was obtained at $M=5.0$ kg/m^3. The condition corresponds to the optimum one reported to obtain a large ZnSe single crystal by using the vertical systems[15], where the transport rate was limited by thermal convection. At $M>5.0$ kg/m^3, the needle-like crystals resulted, the dimensions of which were about 1 mm in diameter and 5 mm in length. In the region of $T_g>1173$ K, some liquid phase appeared in the growth ampoule, but the ZnSe crystals were not obtained.

2.3 Characterization by photoluminescence measurements

The photoluminescence (PL) was measured by using the conventional apparatus shown in Fig. 4. The measurement for the grown crystals was carried out at 4.2 K by using 12 mW He–Cd laser ($\lambda=325$ nm, Liconix) for excitation and a 1-m double monochromator (JASCO,CT1000D) and detected by a photomultiplier followed by lock-in amplifier.

Figures 5a and 5b show the PL spectra of the crystals grown by chemical transport and sublimation, respectively. Fig. 5a only shows a broad band due to the self-activated emission (SA, 2.0 eV)[24], while the excitonic emissions: excitons bound at donor (I_2, 2.797 eV) and acceptor (I_1^d, 2.782 eV) were observed in Fig. 5b.

The results indicate that non-radiative recombination centers were predominant in the crystals by chemical transport. The excess iodine contained in the crystals are considered as non-radiative centers, since the crystals grown in $M>5.0$ kg/m^3 were dark brown and the excess iodine deposited out on the surface after the growth. The electrical resistivity measured for the

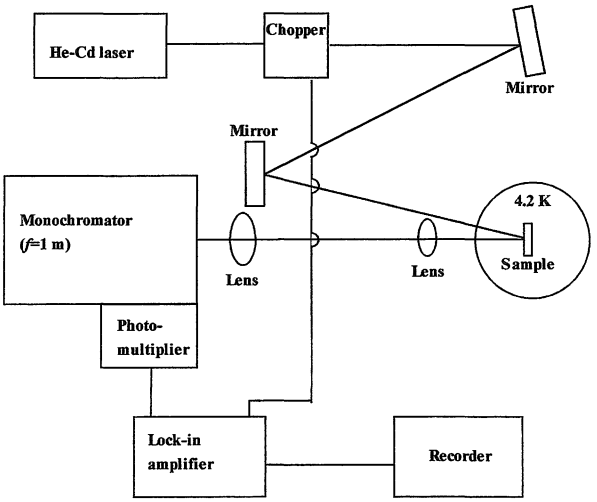

Fig. 4. Schematic diagram of photoluminescence measurement.

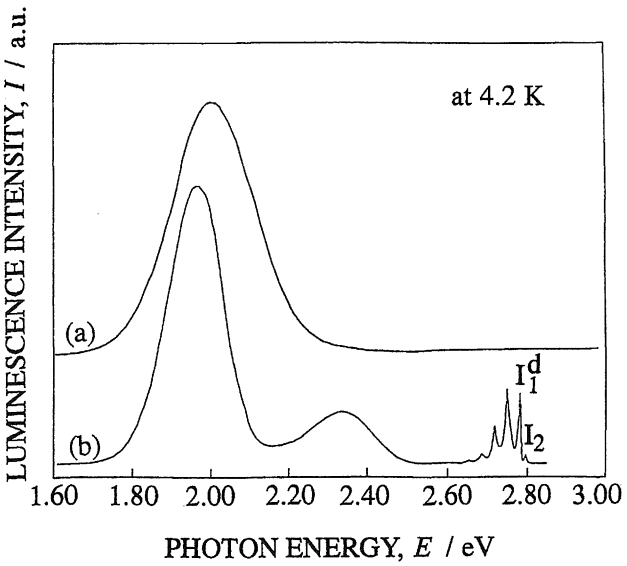

Fig. 5. Photoluminescence spectra of ZnSe crystals grown by (a) chemical transport at $T_s=1098$ K and $\Delta T=25$ K, with $M=5.0$ kg/m^3, and (b) sublimation method. The broad band (peak at 2.0 eV) in (a) is identified as the self-activated emission, and the excitonic emissions in (b) are ascribed to the excitons bound at donor (I_2, 2.797) and acceptor (I_1^d, 2.782 eV).

crystals grown at $M>1.0$ kg/m^3 by using In-dotted contacts was of 10^5 ohm·m-order of magnitude. Although halogen atoms have been reported to act as a donor in the crystal[25], the defects introduced during the growth might have made the crystals insulator. The further heat-treatments such as Zn-dipping might be necessary for the quality enhancement[26].

3. Chemical Transport of $AgGaS_2$

3.1 Experimental

Polycrystalline $AgGaS_2$ was synthesized at 1323 K by direct melting of the constituent elements: Ag (nominal purity of 99.999%), Ga (99.9999%) and S (99.9999%). The poly-crystals (about 1×10^{-3} mol) as a source were sealed with the transport agent into a transparent quartz ampoule (8 mm in inner diameter and 10 cm in length). Metal halides were adopted as the transport agent as well as iodine. The ampoule was heated for four days in a two-zone furnace shown in Fig. 1. The morphology of the as-grown crystals was investigated using a two-circle optical goniometer. The crystal structure was investigated by taking X-ray oscillation photographs using Cu K_α radiation.

3.2 Transport rate by using iodine

The transport parameters affecting crystal growth were: amount of iodine, M=0.1–6.0 kg/m^3; source temperature, T_s=1198–1248 K; temperature difference between source and growth zones, ΔT=25–100 K.

Figure 6 shows the relationship between the transport rate and T_s in terms of ΔT at M=2.0 kg/m^3. The figure indicates two points. One is that the observed transport rate tends to increase with increasing ΔT at a fixed T_s, but a higher transport rate does not necessarily mean bigger single crystals. The other is the presence of a maximum transport rate with increasing T_s at a fixed ΔT. This indicates that the condensation of the atoms at the growth zone was delayed with increasing growth temperature. Figure 7 shows the relationship between the transport rate and M where the peaks were at M=0.3–0.8 kg/m^3. The results indicate that the rate determining process of the transport might be changed from evaporation of the source material to gaseous diffusion with increasing amount of iodine[27].

All the as-grown crystals were transparent-yellow and in rod or block form, which are shown in Fig. 8 and schematically illustrated in Figs. 9a and 9b. The crystal forms were illustrat-

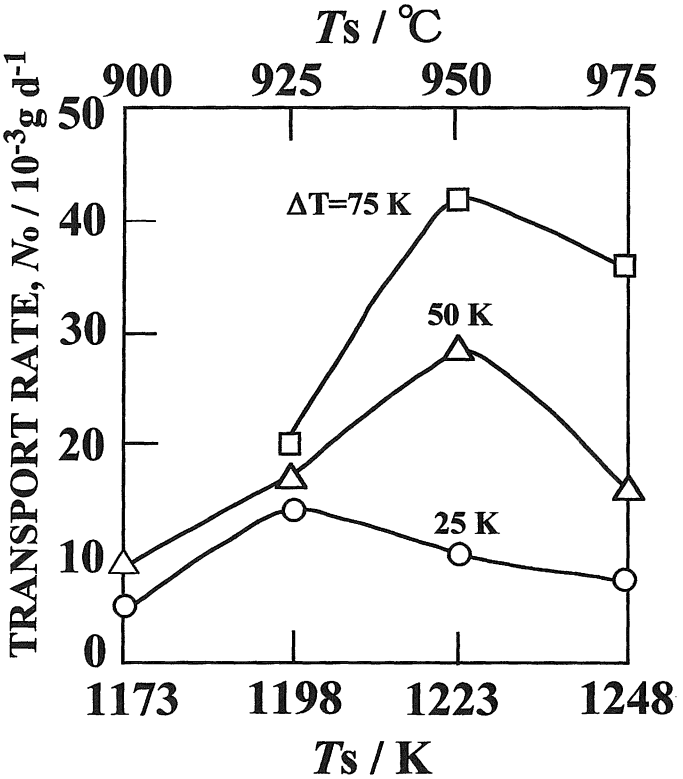

Fig. 6. Plots of the transport rate versus T_s. M=2.0 kg/m^3.

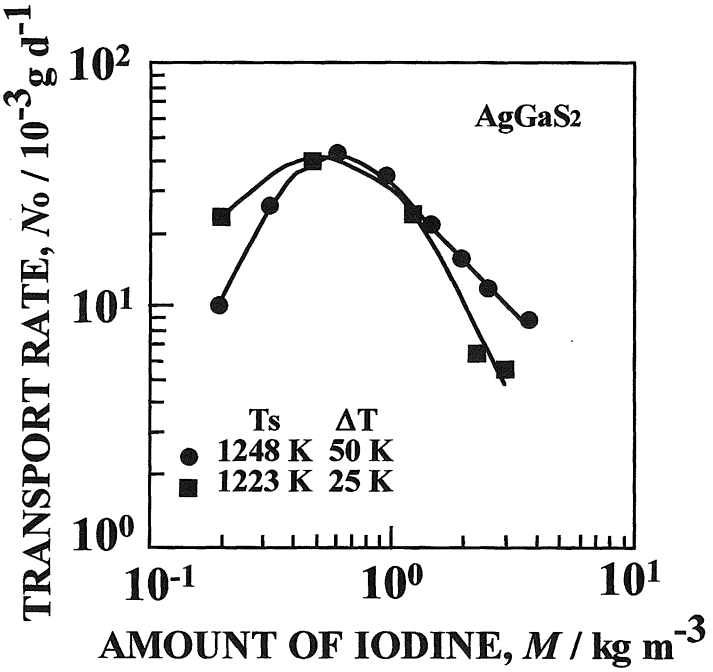

Fig. 7. Plots of transport rate versus M.

ed in Fig. 10 in terms of the growth temperature and the transport rate. The rod single crystals were obtained at the conditions of the growth temperature of more than 1173 K and the transport rate of less than 10 mm/d. The biggest block crystal ($7\times5\times2$ mm^3) was obtained under the conditions (T_s=1248 K, ΔT=75 K, for one week). The habit planes of the rod are illustrated in the (112) stereographic projection in Fig. 9c. The growth direction is nearly in the [113] direction. The block-form crystals have a wide and rippled (112) plane as if the needles were laterally arranged.

3.3 Transport rate by using halides

The transport agents were AgCl, AgBr, $CdBr_2$, and AgI as halogen source. Gallium halides were not used as a transport agent due to their hygroscopic properties. The amount of transport agent was kept at M=0.03–6 kg/m^3, the source temperature was at T_s=1198–1248 K and the temperature difference between source and growth zones was at ΔT=25–100 K. The ampoule was heated for 4–7 days.

The $AgGaS_2$ single crystals grew at the end of the growth zone in the ampoule. All the crystals obtained were transparent yellow and had a block-form with well-developed habit planes, as was stated above. Figure 11 shows the relationships between the transport rate and the amount of the transport agent for the different transport agents. Each curve exhibits a maxi-

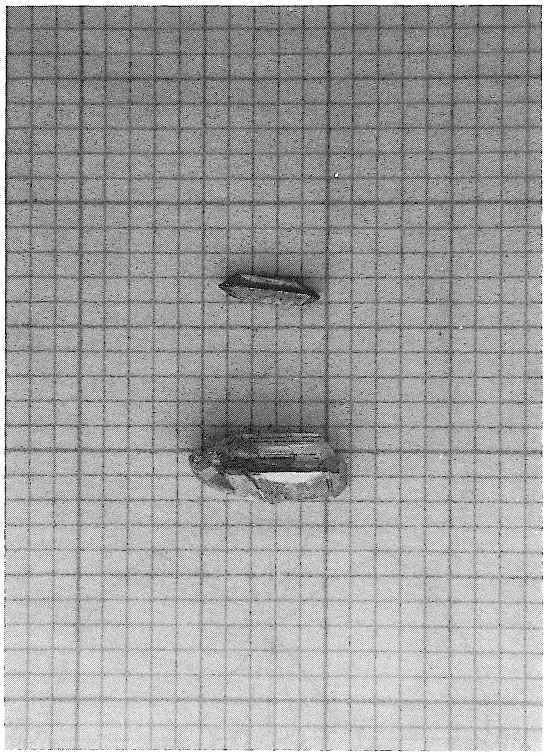

Fig. 8. $AgGaS_2$ crystals grown at $T_s=1248$ K and $\Delta T=50$ K with $M=0.2$(rod) and 1.0(block) kg/m³. 1 div. = 1 mm.

mum in the region of the amount of transport agent 0.3–0.8 kg/m³; the maximum transport rates were 1×10^{-6} kg/d at 0.4 kg/m³ AgCl, 4.0×10^{-6} kg/d at 0.4 kg/m³ AgBr, 5×10^{-6} kg/d at 0.3 kg/m³ $CdBr_2$, and 80×10^{-6} kg/d at 0.3 kg/m³ AgI for $T_s=1248$ and $\Delta T=25$ K.

It is noticed that the maximum growth rate in the case of AgI is about eighty times larger than that of AgCl. The maximum transport rates for the bromides AgBr and $CdBr_2$ are almost equal, with the amount of bromine of 1–2 g-atom/m³. The results indicate that the bromines in the molecules equally contribute to the transport. At $T_s=1223$ K and $\Delta T=25$ K, the maximum transport rate with AgI is twenty times larger than that with AgBr. Thus, it is found that the transport rates increase in order of the transport agent; AgCl, AgBr ($CdBr_2$), and AgI(iodine). Table 1 lists the values of heat of formation (H_0^{298})[28]. From the point of view of the reaction between halogen atoms and the constituent elements, it should be pointed out that the order of the transport rate corresponds to that of H_0^{298} of gaseous Ag- and Ga-halides. The thermodynamic analysis is left for further studies. The relationship between the transport rate and the amount of iodine is steep on both sides of the maximum transport rate as shown in Fig. 7, which is different from the results obtained in Fig. 11 by using the halides.

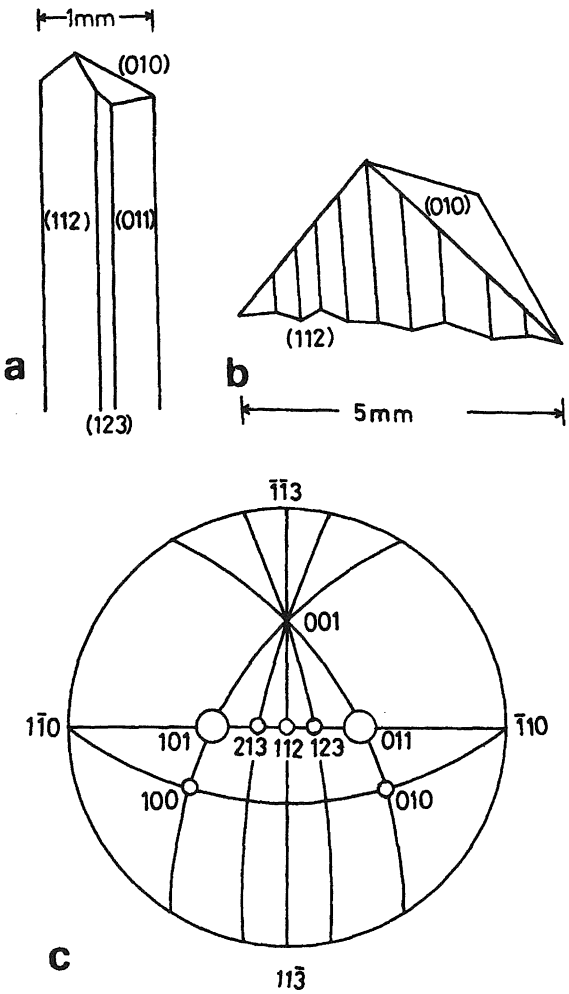

Fig. 9. Schematic of $AgGaS_2$ crystals: (a) rod, (b) block and (c) (112) stereographic projection ($c/a=1.79$) of the rod. Circles indicate habit planes of the rod.

3.4 PL spectra

The emission spectrum was measured at 4.2 K using the same apparatus shown in Fig. 4 with He–Cd laser excitation ($\lambda=441.6$ nm). The direct comparison of different data was made by keeping the laser power (20 mW), the irradiated area (1×1 mm^2) on the crystal surface and the detection sensitivity constant.

Figure 12 shows the PL spectrum of the single crystal grown using 0.18 kg/m^3 iodine. The emission energies of 2.699, 2.695 and 2.687 eV correspond to those which had been attributed to (i) the free exciton (E_x), (ii) the bound excitons to the neutral donor (I_2) and (iii) the neu-

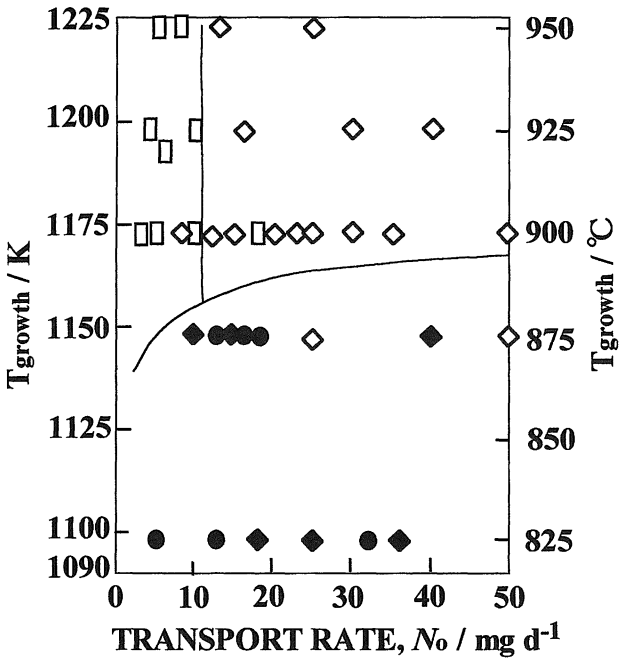

Fig. 10. Crystal forms plotted in terms of growth zone temperature and transport rate. (□): rods; (◇): block; (◆): polycrystal; (●): fine crystal.

tral acceptor (I_1)[3)29-31)], respectively. The result indicates that a good quality crystal was obtained with dominant radiative recombination.

The PL spectra are shown in Fig. 13 for the cases of M=0.18, 0.79, 2.09 and 3.53 kg/m^3 at T_s=1248 K and ΔT=25 K. The blue peak (at 2.632 eV) and the green band (peak at 2.48 eV) were observed for the crystal grown with M=0.18 kg/m^3, which were reported previously[30-34)] and attributed to Ag and Ga vacancies, respectively[35)].

With increasing M, the excitonic emissions disappeared. The crystals grown with more than 5.0 kg/m^3 iodine became opaque in a month and no emission could be detected. Thus the iodine in the crystal seems to cause some non-radiative center. Since the observation of the excitonic emission indicates a good quality of crystal, the amount of iodine must be limited in the range from 0.2 to 2.0 kg/m^3 to obtain high-quality single crystals.

It was also found that the intensity of the green emission was much larger than that of the blue emission and that consequently, the Ga vacancy was predominant in the crystals grown by the chemical transport. The emission intensity of E_x in the iodine-transport crystals was plotted in Fig. 14 as a function of the amount of iodine. The ratios (I/I_{EX}) of the intensities of the blue and the green lines to that of E_X were plotted in Fig. 15. The least squares fit provides a linear relationship between the intensity and the amount of iodine, as shown by solid lines in these

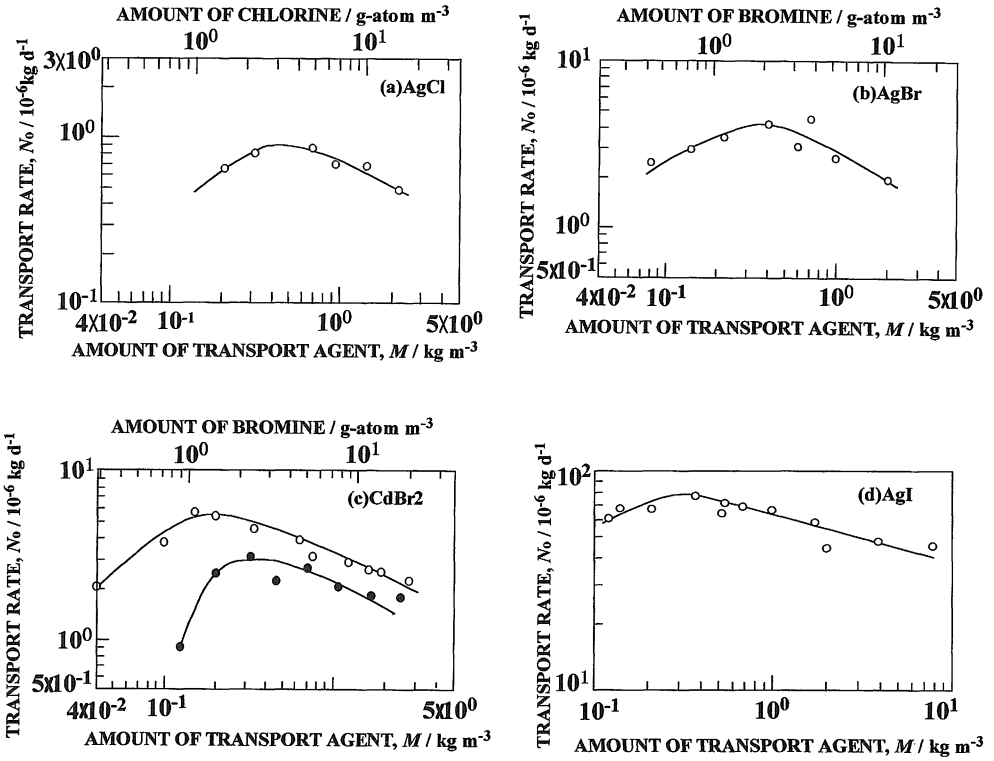

Fig. 11. Plots of transport rate versus amount of transport agent. Transport agent: (a) AgCl at T_s=1248 K and ΔT=25 K, (b) AgBr at T_s=1248 K and ΔT=25 K, (c) $CdBr_2$ at T_s=1248 K(○) and 1123 K(●) with ΔT=25 K, (d) AgI at T_s=1248 K and ΔT=25 K.

Table 1 Heat of formation (H_0^{298} in kcal/mol) for gaseous Ag– and Ga–halides[28].

Halogen(X)	AgX	GaX_3	GaX
Cl	+23.2	−102	−20
Br	+29	−72	−8
I	+33	−28	+10

(1 kcal/mol=4.1840×10³ J/mol)

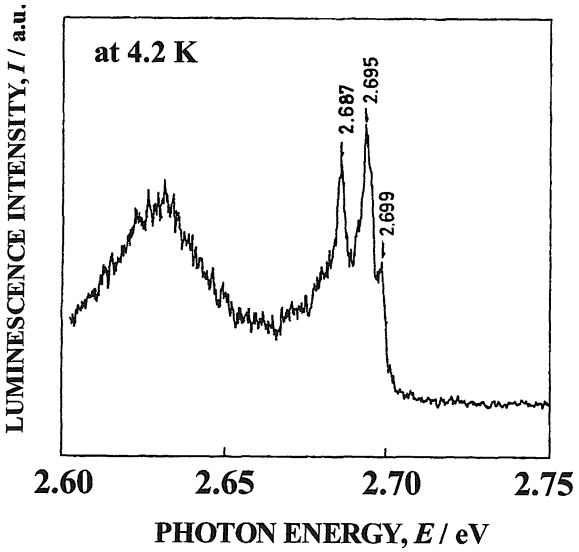

Fig. 12. Excitonic emissions of a $AgGaS_2$ single crystal grown with M=0.18 kg/m³.

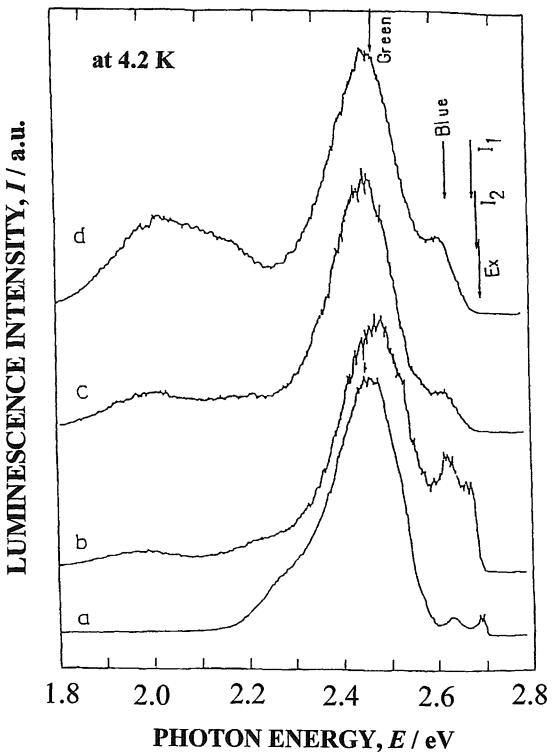

Fig. 13. Photoluminescence spectra of $AgGaS_2$ single crystals grown at T_s=1248 K and ΔT=25 K using iodine. The amounts of iodine are (a) 0.18, (b) 0.79, (c) 2.09 and (d) 3.53 kg/m³ respectively.

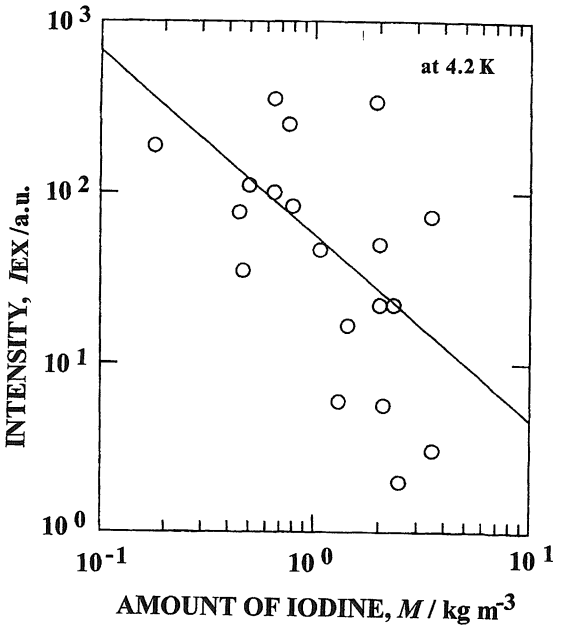

Fig. 14. Plots of intensity of E_x versus amount of iodine.

figures. Despite the considerable scatter of the data, the intensity of the E_x tends to decrease with an increase of iodine. This indicates that nonradiative recombination centers were introduced with an increase of iodine. The intensity ratios of blue and green to E_x increased with an increase of iodine, showing the same inclination, which was equal to the inverse of that for E_x. This fact indicates that nonradiative recombination centers were introduced into the grown crystals, while the intensities of the blue and green lines were almost independent of the amount of iodine. The nonradiative centers may be assigned either to impurities such as halogen atoms or to the lattice defects due to the deviation from the stoichiometric composition.

Figure 16 shows the PL spectra of crystals obtained by using $CdBr_2$. The characteristic features of the spectra in the case of $CdBr_2$-grown crystals were as follows. (i) The E_x peak was not found for the crystals obtained by using even small amounts of $CdBr_2$ (Fig. 16a). This fact suggests that much more non-radiative recombination centers were introduced into the $CdBr_2$-grown crystals than into the iodine-grown ones. (ii) Two new peaks were found at 2.679 and 2.613 eV, which were close to the energies of the I_1 and the blue lines, respectively (Fig. 16b). (iii) The green line was observed similarly as in the case of iodine-grown crystals. Since the blue and the green lines have been assigned to the Ag and the Ga vacancies, respectively[35], the results (ii) and (iii) suggest the incorporation of Cd atoms into the crystal to form recombination centers resulting in another blue emission line.

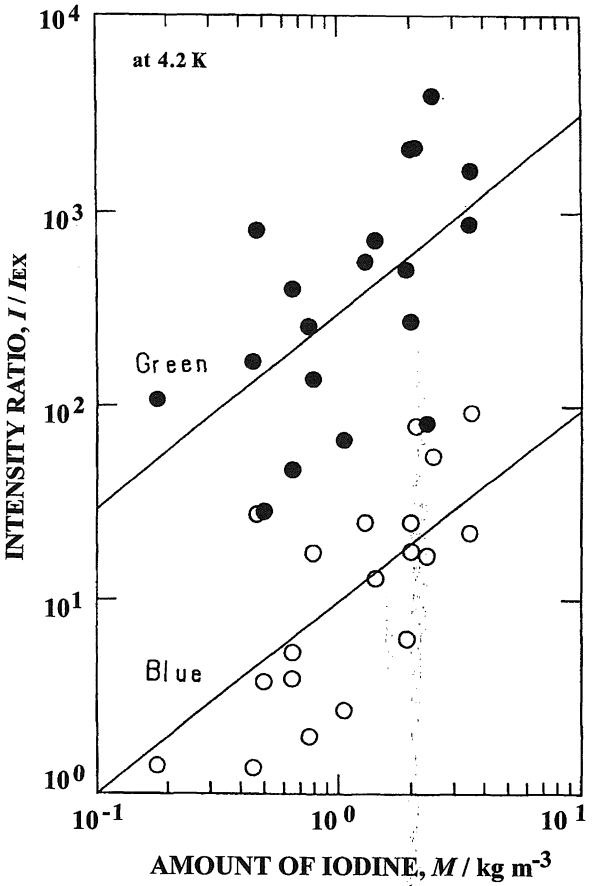

Fig. 15. Plots of intensity ratios (I/I_{EX}) of blue (○) and green (●) emissions versus amount of iodine.

4. Summary

(1) The chemical transport rates of ZnSe and $AgGaS_2$ were experimentally measured by using iodine and halides as the transport agent in a horizontal closed ampoule. The transport rate was measured as a function of M and in terms of transport agent.

(2) The morphologies of the grown crystals were classified in terms of the growth conditions, where the conditions to obtain large size crystals indicated.

(3) The crystals were estimated by measuring photoluminescence spectra. In case of ZnSe, the PL spectra only showed the SA emission, while non-radiative recombination centeres were introduced with an increase of transport agent in $AgGaS_2$. The results suggests that non-radiative recombination centers might inevitably be introduced during transport process leading to poor quality.

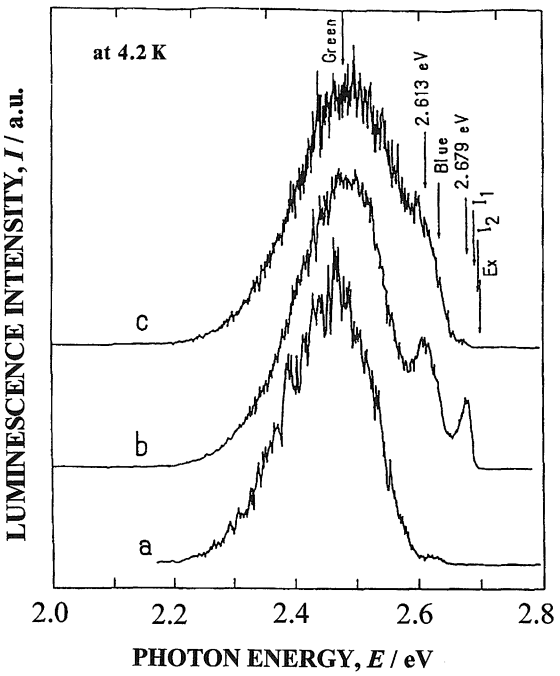

Fig. 16. Photoluminescence spectra of $AgGaS_2$ Single crystals grown at $T_s=1248$ K and $\Delta T=25$ K by using $CdBr_2$. The amount of $CdBr_2$ is (a) 0.04, (b) 0.20 and (c) 0.63 kg/m^3, respectively.

(4) The quality must be enhanced by further heat-treatments.

(5) The transport rate in the chemical transport has been explained on the basis of diffusion processes of gaseous molecules. Thermodynamical considerations are left in the further studies to understand the transport process.

References

1) M. A. Haase, J. Qiu, J. M. DePuydt: Appl. Phys. Lett., **59**(1991), 1272.
2) J. L. Shay and J. H. Wernick: *Ternary Chalcopyrite Semiconductors, Growth, Electronic Properties and Applications,* (Pergamon, Oxford, 1975).
3) B. Tell and H. M. Kasper: Phys. Rev., **B4** (1971), 4455.
4) M. V. Hobden: Acta Cryst., **A24** (1968), 676.
5) V. M. Cound, P. H. Davis, K. F. Hulme and D. Robertson: J. Phys., **C3** (1970), L83.
6) D. S. Chemla, P. J. Kupecek and D. S. Robertson: Opt. Commun., **3** (1971), 29.
7) G. D. Boyd, H. Kasper and J. H. McFee: IEEE J. Quant. Electron., **QE-7** (1971), 563.
8) R. S. Feigelson and R. K. Route: Opt. Eng., **26** (1987), 113.
9) S. Wagner: J. Appl. Phys., **45** (1972), 246.
10) S. Shionoya: *Kessho Kogaku Handbook* (in Japanese), (Kyoritsu Shuppan, 1971), p. 699.

11) H. Yoshida, T. Fujii, A. Kamata and Y. Nakata: J. Cryst. Growth, **117** (1992), 75.
12) T. Kiyosawa, K. Igaki and N. Ohashi: Trans. JIM., **13** (1972), 248.
13) R. Nitsche: J. Phys. Chem. Solids, **17** (1960), 163.
14) M. Aoki, M. Washiyama, H. Nakamura and K. Sakamoto: Jpn. J. Appl. Phys. Suppl., **21–1** (1982), 11.
15) E. Kaldis: *Crystal Growth, Theory and Techniques,* Vol. 1, ed by C. H. L. Goodman, (Plenum, New York, 1974), p. 49.
16) R. S. Feigelson and R. K. Route: Opt. Eng., **26** (1987), 113.
17) R. Korczak and C. B. Staff: J. Cryst. Growth, **24/25** (1974), 386.
18) R. S. Feigelson: J. Phys., **C3** (1975), 57.
19) H. Matthes, R. Viehmann, N. Marschall and P. Korczak: J. Phys., **C3** (1975), 105.
20) R. K. Route, R. J. Raymakers and R. S. Feigelson: J. Cryst. Growth, **29** (1975), 125.
21) N. B. Singh, P. H. Hopkins and J. D. Feichtner: J. Mater. Sci., **21** (1986), 837.
22) W. H. Honyman and K. H. Wilkinson: J. Phys., **D4** (1971), 1182.
23) H. A. Chedzey, D. J. Marshall, H. T. Parfitt and D. S. Robertson: J. Phys., **D4** (1971), 1320.
24) S. Iida: J. Phys. Soc. Japan, **25** (1968), 177.
25) J. I. Pankove: *Electroluminescence*, (Springer-Verlag, Berlin, 1977), p. 141.
26) M. Aven and H. H. Woodbury: Appl. Phys. Lett., **1**(1962), 53.
27) T. Arizumi and T. Nishinaga: Jpn. J. Appl. Phys., **4** (1965), 165.
28) E. Sirtl: Z. Naturforsch., **21a** (1966), 2001.
29) J. P. Noblanc, J. Loudette, G. Duraffourg and D. S. Robertson, Appl. Phys. Lett., **20** (1972), 257.
30) J. P. Aicardi, J. P. Leyris and A. Poure: J. Appl. Phys., **53** (1982), 1690.
31) J. P. Aicardi and G. Aguerro: Phys. Stat. Sol., **(a)95** (1986), 679.
32) P. W. Yu and Y. S. Park: J. Appl. Phys., **45** (1974), 823.
33) G. Auguero, J. P. Aicardi and J. P. Leyris: J. Phys., **42** (1981), 317.
34) G. Massé and E. Redjai: J. Lumin., **33** (1985), 369.
35) Y. Noda, T. Kurasawa, H. Watanabe, Y. Furukawa and K. Masumoto: *Non-stoichiometry in Semiconductors*, ed. K. J. Bachmann, H.-L. Hwang and C. Schwab, (Elsevier, 1992), p. 63.